Supplemental methods

Endothelial cell culture. Human aortic endothelial cells (HAEC) were obtained from Clonetics and cultured in endothelial basal medium (Clonetics) supplemented with growth factors in a humidified atmosphere (37°C, 95% air / 5% CO2). HAECS were grown to confluence and rendered quiescent before experiments by incubation in medium containing 0.5% FCS. Mouse aortic endothelial cells (MAEC) were obtained by collagenase digestion of aorta from C57BL/6 wild type mice. In brief, the aorta was excised, filled with 0.2% Collagenase/Dispase (Roche) and incubated for 30 min at 37°C. Afterwards the aorta was rinsed with HBSS washing buffer (1x HBSS w/o calcium and magnesium, 1 mM HEPES, 0.1 % BSA). The eluted cells were centrifuged and plated on 12 cm dishes in DMEM (Gibco) containing 20% FCS and endothelial cell growth supplements.

Measurement of endothelial cell nitric oxide (NO) production by electron spin resonance spectroscopy. The effects of HDL (50 μg/ml; 60 min, 37°C) on endothelial NO production (HAECs; passage 4-7; Cambrex Bio Science) was examined by electron spin resonance (ESR) spectroscopy using the spin-probe colloid $Fe(DETC)_2$ (Noxygen), as described and validated previously[1-4]. In brief, ESR spectra of samples frozen in liquid nitrogen were recorded on a Bruker e-scan spectrometer (Bruker BioSpin) with the following instrumental settings: center field (B0) 3455 G, sweep width 80 G, microwave power 39.72 db, amplitude modulation 10.34 G, sweep time 10.49 sec, number of scans 10. Separate experiments were performed to examine the effects of NO synthase inhibitor

NG-nitro-L-arginine methyl ester (L-NAME, 1 mM, Sigma-Aldrich) and *eNOS*-specific siRNA (Sigma-Aldrich). After incubation with the NO synthase inhibitor L-NAME and siRNA-induced knockdown of eNOS expression, no NO-specific ESR signal was detected, indicating that the ESR signal was specific for NO (data no shown).

Measurement of endothelial cell NO production by 4,5-diaminofluorescein diacetate (DAF-2) staining. Human aortic endothelial cells were seeded on six-well plates and cultured in endothelial basal medium supplemented with growth factors (according to the manufacturer`s instructions; Clonetics). Endothelial cell NO production was determined as described in detail previously[5, 6]. In brief, after overnight starvation in medium containing 0.5% FCS, cells were incubated for one hour at 37°C with HDL (50 µg/ml) and DAF-2 diacetate (1 µM; Cayman Chemical), that forms the fluorescent triazolofluorescein upon reaction with cellular NO. Following incubation, cells were washed twice with EDTA, trypsinized and transferred to a black microplate. Fluorescence was measured in a fluorescence microplate reader using an excitation wavelength of 485 nm.

Measurement of endothelial cell superoxide production by electron spin resonance spectroscopy. The effect of HDL on endothelial cell superoxide production was assessed in unstimulated and TNFα-stimulated (5 ng/ml, R&D Systems) HAECs by ESR spectroscopy, as described in detail previously [1, 2, 7]. Briefly, HAECs were incubated with HDL (50 µg/ml, 60 min, 37°C) with or without TNFα and resuspended in Krebs-Hepes buffer (pH 7,4; Noxygen) containing diethyldithiocarbamic acid sodium salt (5 µM,

Noxygen) and deferoxamine methanesulfonate salt (25 μM, Noxygen). ESR spectra were recorded after addition of the spin probe 1-hydroxy-3-methoxycarbonyl-2,2,5,5-tetramethylpyrrolidine (CMH; Noxygen; final concentration 200 μM) under stable temperature conditions using a Bruker e-scan spectrometer (Bruker Biospin). The ESR instrumental settings were as follows: center field (B0) 3495 G, field sweep width 10.000 G, microwave frequency 9.75 GHz, microwave power 19.91 mW, magnetic field modulation frequency 86.00 kHz, modulation amplitude 2.60 G, conversion time 10.24 msec, detector time constant 328 msec, nuber of x-scans 10.

Measurement of NAD(P)H oxidase activity in endothelial cells by electron spin resonance spectroscopy. The effect of HDL on NAD(P)H oxidase activity was examined in human aortic endothelial cells, as described previously [1, 2, 7]. Endothelial cells were homogenized in 250μl PBS (4°C) containing antiproteolytic agents (CompleteMini, Merck), centrifuged for 10 minutes (4°C), and supernatants were stored on ice until use. Homogenates were added to reaction buffer containing the spin trap 1-hydroxy-3-carboxy-pyrrolidine (CP-H, Noxygen). Measurements were started after addition of 100 μmol/l NADH (Sigma) in 50μl glass capillaries. Superoxide formation was determined following the oxidation of CP-H to paramagnetic 3-carboxy-proxyl for 300 seconds.

Endothelial Monocyte Adhesion. Human monocytes were separated by magnetic cell sorting with CD14 antibodies (Miltenyi Biotec) from peripheral blood mononuclear cells of a healthy human volunteer isolated by Ficoll density gradient centrifugation (Vacutainer CPT, Beckton-Dickinson). Isolated human monocytes were resuspended in

RPMI 1640 containing 10% serum (Gibco) and labelled with carboxyfluorescein diacetate succinimidyl ester (CFSE, Molecular Probes/Invitrogen). HAECs were cultured to confluency in 24-well plates as described above and incubated with HDL (50 μg/ml) for 1 hour. Afterwards, TNFα (1 ng/ml) was added to the medium and HAECs were further incubated for 3 hours. After medium was changed, human monocytes (50.000/well) were added to the HAEC monolayer and incubated for 3 hours in a humidified atmosphere (37°C, 95% air / 5% CO2). Non-adherent cells were removed by washing wells with phosphate buffered saline (PBS, Gibco) and HAECs were counterstained with 4',6-diamidino-2-phenylindole (DAPI) suspended in mounting medium (Dako). Adherent CFSE-labeled monocytes were counted on 4 randomly selected high-power fields using a fluorescent microscope (DM-IRB; Leica) connected to a digital imaging system (Spot-RT; Diagnostic Instruments/Visitron Systems) and normalized to the number of HAECs present on each field.

Western Blot Analyses. Phosphorylation of endothelial nitric oxide synthase (eNOS) at serine residue 1177 and threonine residue 495, phosphorylation of Akt at threonine residue 473, phosphorylation of PKCßII at serine residue 660 and expression of vascular cell adhesion molecule (VCAM)-1 in HAECs were determined by Western Blot analysis. Anti-human phospho-eNOS (Ser1177), anti-human phospho-eNOS (Thr495) and anti-human total-eNOS antibodies were purchased from BD Transduction Laboratories. Antibodies against human phospho-Akt (Thr473) and human total-Akt were from Cell Signaling and the antibody against human VCAM-1 was from R&D Systems. Anti-

human phospho-PKCßII (Ser660) and anti-human total-PKCßII antibodies were purchased from Santa Cruz Biotechnology.

Endothelial Cell Transfection with eNOS specific small interference RNA. Small interfering RNA targeted to *eNOS* and nontargeting scrambled RNA duplex were obtained from Sigma-Aldrich. HAECs grown on 12 well plates were transfected with *eNOS*-specific or scrambled siRNA at a final concentration of 15 nM using the N-TER nanoparticle siRNA transfection system (Sigma-Aldrich) and serum-free cell culture medium according to the manufacturer`s protocol. The siRNA sequence (sense strand) used for targeting human *eNOS* was 5´-CCUACAUCUGCAACCACAU-3´ (predesigned Mission siRNA database, siRNA ID: SASI_Hs01_00174421). The sequence of the sense strand of scrambled siRNA used as a control was 5`-GAUCAUACGUGCGAUCAGA-3´. All siRNA transfections were performed for 24 hours preceding subsequent HAEC measurements.

Detection of nuclear translocation of NF-κB subunit RelA/p65 by immunocytochemistry and quantification of DNA-bound p65 in nuclear extracts of endothelial cells. HAECs were treated for 3 hours with TNFα (1 ng/ml) and nuclear translocation of NF-κB subunit RelA/p65 was detected by staining cells with mouse anti-RelA/p65 (Santa Cruz Biotechnology). Cytoplasmic RelA/p65 was analyzed using a SP2 confocal microscope (Leica), and quantification was performed with the open-source software CellProfiler (www.cellprofiler.org). Intensity of the green channel was

measured in the cytoplasm (nuclear area subtracted from the total cell area) of at least 150 cells per treatment group at the Z-section where the nuclei had their largest diameter.

To confirm the results of the immunocytochemistry approach, we prepared nuclear extracts of HAECs stimulated for 3 hours with TNFα (1 ng/ml) using the Nuclear Extract kit (ActiveMotif) as described previously[8]. Binding of activated NF-κB in the nuclear extracts to an oligonucleotide containing an NF-κB consensus binding site was detected by a RelA/p65 transcription factor assay (TransAM kit, ActiveMotif), as described previously [9].

Binding of HDL to Endothelial Cells. Binding of HDL to human aortic endothelial cells was examined as described in detail previously[1, 10]. In brief, HDL was iodinated with $Na^{125}I$ by the McFarlane monocholoride procedure as modified for lipoproteins. Specific activities of approximately 300-700 cpm/ng of protein were obtained. Interactions of ^{125}I-HDL (5 μg/ml, 50 min) with endothelial cells were examined and specific binding was calculated by subtracting the values of the non-specific binding from those of the total binding as described previously. To examine the functional relevance of SR-BI for the specific endothelial binding of HDL from healthy subjects and patients with CAD, SR-BI expression in endothelial cells was inhibited by SR-BI specific siRNA knockdown as described previously[10]. Endothelial cells were transfected with 100 nM Stealth siRNA (Invitrogen) against SR-BI (sequence, sense strand: TCGTCATGCCCAACATCCTGGTCTT) or non-coding scrambled siRNA (sequence, sense strand: AGAGCTTATCCCTC-GGTTGTGTCGT) with Lipofectamine 2000 (Invitrogen) in OPTIMEM according to the manufacturer's protocol. 6 h after

transfection, the medium was replaced by DMEM 5% FCS. Binding assays were conducted between 60 and 72 h after transfection. The efficiency of the silencing was evaluated by quantitative RT-PCR and Western-blotting.

Characterization of cellular cholesterol efflux capacity of HDL. Total and ABCA1-dependent efflux of [^{14}C]cholesterol to HDL was measured using J774 macrophages treated with or wihout the cAMP analogue 8-(4-chlorophenylthio) adenosine 3′:5′-cyclic monophosphate (cpt-cAMP) to induce ABCA-1 expression, as described previously[11, 12]. On day 0, J774 macrophages were plated in 24-well plates at density of 2×10^5 cells/well in DMEM (high glucose) with 10 % (v/v) FBS and antibiotics. On day 1 cells were labeled with 0.5 ml of labeling medium (8 μCi/ml 4[^{14}C]cholesterol in DMEM (high glucose) supplemented with 0.2 % (w/v) bovine serum albumin (BSA)). Following 24 h of labeling and washing, cells were equilibrated for 24 h with or without 0.3 mM cpt-cAMP in 0.5 ml of DMEM (high glucose) supplemented with 0.2 % (w/v) BSA. At the end of the treatment period with cpt-cAMP, cells were washed twice and incubated with 0.5 ml of DMEM (high glucose) supplemented with 0.2 % (w/v) BSA, with or without HDL (10 μg/ml apoA-I) at 37°C for 4h. The radioactivity in 40 μl of the supernatant was determined by liquid scintillation counting. At the end of the incubation, cells were lysed in 400 μl of lysis buffer (PBS containing 1 % (v/v) Triton X-100) for 30 min at room temperature and radioactivity was measured in 40 μl cell lysate. The percentage of secreted [^{14}C]cholesterol was calculated by dividing the medium-derived counts by the sum of the total counts present in the culture medium and the cell lysate. To calculate the

ABCA1-dependent efflux, the cholesterol efflux of the untreated cells was subtracted from the cholesterol efflux of the cells treated with cpt-cAMP.

ABCG1-dependent cholesterol efflux capacity of HDL was measured in HEK293 cells transfected with an ABCG1-expressing plasmid or a mock plasmid, as described previously[11]. In brief, HEK293 cells were cultured in DMEM (high glucose) with 10% (v/v) FBS and antibiotics. One day before transfection, the cells were plated on 24-well plates coated with poly-d-lysine at density of 2×10^5 cells/well in the same medium without antibiotics. The next day, cells at about 95% confluence were transfected with LipofectAMINE 2000 and ABCG1 or pcDNA1 (mock) plasmids for 16 h. The DNA-LipofectAMINE 2000 complexes were formed in serum-free Opti-MEM I. After this period of time, cells were labeled with 1 μCi/ml 4-[^{14}C]cholesterol in DMEM (high glucose) supplemented with 10% (v/v) FBS. Following 24 h of labeling, cells were washed twice with PBS and incubated for 1 h with DMEM (high glucose) supplemented with 0.2% (w/v) fatty acid-free BSA. At the end of this period, cells were incubated with 0.5 ml of DMEM (high glucose) and supplemented with 0.2% (w/v) fatty acid-free BSA with or without HDL (28 μg/ml apoA-I) at 37 °C for 4 h. The media were collected and clarified by centrifugation in a microcentrifuge for 2 min, and the radioactivity in 300 μl of the supernatant was determined by liquid scintillation counting. The cells were lysed with 0.5ml 0.1 M NaOH, and the radioactivity in a 300-μl aliquot of the cell lysate was determined by scintillation counting. [^{14}C]cholesterol efflux was expressed as the percentage of the radioactivity released in the medium relative to the total radioactivity in cells and medium. To calculate the net ABCG1-mediated efflux, the cholesterol efflux of

the cells transfected with the control plasmid (mock) was subtracted from the cholesterol efflux of the cells transfected with the ABCG1 plasmid.

Detection of membrane translocation of PKCβII. To examine membrane translocation of PKCßII, cytosol and membrane fractions of human aortic endothelial cells were prepared as follows. Endothelial cells were incubated in a lysis buffer containing 50 mmol/l HEPES (pH 7.4), 50 mmol/l NaCl, 1 mmol/l $MgCl_2$, 2 mmol/l EDTA, 1 mmol/l PMSF, 10 mg/ml leupeptin, 1 mmol/l $NaVO_4$, and 0.1% Triton X-100 for 5 minutes on ice. The cell lysates were centrifuged at 15 000 rpm and 4°C for 15 minutes. After the supernatant had been collected as the cytosol fraction, the pellet was resuspended in 1% Triton X-100 in the lysis buffer and centrifuged at 15 000 rpm and 4°C for 15 minutes. The supernatant was then collected as the membrane fraction. Equal amounts (25 µg) of protein from each fraction were subjected to SDS-polyacrylamide gel electrophoresis followed by immunoblotting with anti-human total-PKCbeta-2 antibodies (Santa Cruz Biotechnology), as described above.

Proteolytic digestion of HDL and LC-ESI-MS/MS analysis. Native or carbonyl-modified HDL was digested with sequencing grade modified trypsin (Promega) or sequencing grade endoproteinase Glu-C (Roche Applied Science) and fractionated by LC. MS/MS analyses were performed on a hybrid LTQ-Orbitrap mass spectrometer (ThermoFischer Scientific) interfaced with a nano-electrospray ion source. For quantification, reconstructed ion chromatograms were derived from 3 peptides carrying the lysine-MDA modifications normalized to the reconstructed ion chromatograms of the

most abundant peaks in the survey scan. Based on this method, only apolipoprotein A1-specific peptides were found to carry MDA-lysine adducts. The following lysine-MDA containing peptides were taken for reconstructed ion chromatograms: LYRQ(K+54)VEPLRAE, SF(K+54)VSFLSALEE, YHA(K+54)ATEHLSTLSE. The average of the normalized values was taken for comparison across treatment groups.

Measurement of PON1 activity and content of HDL. Paraoxonase and arylesterase activities of HDL-associated paraoxonase were independently measured within one day after HDL isolation by UV spectrophotometry in a 96-well plate format (Nunclon Surface, Nunc, Roskilde, Denmark) using paraoxon (Sigma-Aldrich) or phenyl acetate (Sigma-Aldrich) as substrates, as previously described[13]. For arylesterase assays, HDL (100 μg protein/well) was dissolved in a reaction mixture of 9mM Tris hydrochloride (pH 8.0) and 0.9mM calcium chloride. The reaction was initiated at 24°C by addition of 3.4 mM phenylacetate and the increase in absorbance at 270 nm was recorded. Arylesterase activity was calculated from the molar extinction coefficient of 1310M-1 • cm-1 (at 270 nm) and expressed as the amount of phenyl acetate hydrolyzed in micromoles per minute per microgram of HDL. For paraoxonase activity assays, HDL was diluted in reaction mixture containing 10mM Tris hydrochloride (pH 8.0), 1 M sodium chloride and 2 mM calcium chloride. The reaction was initiated at 24°C by addition of 1.5 mM paraoxon and the increase in absorbance at 405nm due to the generation of para-nitrophenol was recorded. An extinction coefficient of 17.000 M-1 • cm-1 (at 24°C) was used for calculating units of paraoxonase activity, which are expressed as the amount of para-nitrophenol produced in nanomoles per minute per milligram of HDL. Paraoxonase and

arylesterase assays for each sample were performed in triplicates and average measurements of enzyme activity were calculated for each sample. Each 96-well plate included blank samples to monitor spontaneous hydrolysis of substrates. PON1 content was measured by Western Blot analysis. Briefly, HDL (50 μg/ml) was separated by SDS-PAGE (10-20% gradient gels), transferred onto PVDF membranes, and probed using an affinity isolated antibody to PON1 (Sigma-Aldrich).

Inhibition of PON1 and supplementation of HDL with purified human PON1. HDL-associated PO-1 was inhibited by the specific PON1 inhibitor hydroxyquinoline[14, 15] or EDTA. HDL isolated from healthy subjects (100 μg of protein/ml) was incubated for 3 h at 37 °C with either Krebs-Henseleit buffer alone (Control-HDL), or the PON1 specific inhibitor 2-hydroxyquinoline (200 μM), or Na_2EDTA (5 mM) dissolved in Krebs-Henseleit buffer. After the incubation period, HDL was dialyzed to remove remaining amounts of HQ or EDTA and was then directly used for the in vivo and in vitro studies. Measurements of paraoxonase activity following dialysis revealed an inhibition of PON1 by 78±9% ($P<0.01$) after incubation with 2-hydroxyquinoline and 71±12% ($P<0.01$) after incubation with EDTA.

To further determine the role of HDL-associated PON1 activity for the endothelial effects of HDL, HDL from PON1 deficient mice or HDL from patients with CAD was supplemented with purified human PON1, that was isolated as described previously[16]. PON1 was supplemented at a dose of 5 U/100 μg HDL protein, representing a similar paraoxonase activity as observed in HDL from healthy subjects.

References

1. Sorrentino SA, Besler C, Rohrer L, et al. Endothelial-vasoprotective effects of high-density lipoprotein are impaired in patients with type 2 diabetes mellitus but are improved after extended-release niacin therapy. *Circulation.* Jan 5 2010;121(1):110-122.

2. Sorrentino SA, Bahlmann FH, Besler C, et al. Oxidant stress impairs in vivo reendothelialization capacity of endothelial progenitor cells from patients with type 2 diabetes mellitus: restoration by the peroxisome proliferator-activated receptor-gamma agonist rosiglitazone. *Circulation.* Jul 10 2007;116(2):163-173.

3. Kleschyov AL, Munzel T. Advanced spin trapping of vascular nitric oxide using colloid iron diethyldithiocarbamate. *Methods Enzymol.* 2002;359:42-51.

4. Khoo JP, Alp NJ, Bendall JK, et al. EPR quantification of vascular nitric oxide production in genetically modified mouse models. *Nitric Oxide.* May 2004;10(3):156-161.

5. Nakatsubo N, Kojima H, Kikuchi K, et al. Direct evidence of nitric oxide production from bovine aortic endothelial cells using new fluorescence indicators: diaminofluoresceins. *FEBS Lett.* May 8 1998;427(2):263-266.

6. Leikert JF, Rathel TR, Muller C, et al. Reliable in vitro measurement of nitric oxide released from endothelial cells using low concentrations of the fluorescent probe 4,5-diaminofluorescein. *FEBS Lett.* Oct 5 2001;506(2):131-134.

7. Hilfiker-Kleiner D, Kaminski K, Podewski E, et al. A cathepsin D-cleaved 16 kDa form of prolactin mediates postpartum cardiomyopathy. *Cell.* Feb 9 2007;128(3):589-600.

8. Binder NB, Niederreiter B, Hoffmann O, et al. Estrogen-dependent and C-C chemokine receptor-2-dependent pathways determine osteoclast behavior in osteoporosis. *Nat Med.* Apr 2009;15(4):417-424.

9. Stein S, Schafer N, Breitenstein A, et al. SIRT1 reduces endothelial activation without affecting vascular function in ApoE-/- mice. *Aging (Albany NY).* Jun 2010;2(6):353-360.

10. Rohrer L, Ohnsorg PM, Lehner M, et al. High-density lipoprotein transport through aortic endothelial cells involves scavenger receptor BI and ATP-binding cassette transporter G1. *Circ Res.* May 22 2009;104(10):1142-1150.

11. Chroni A, Liu T, Gorshkova I, et al. The central helices of ApoA-I can promote ATP-binding cassette transporter A1 (ABCA1)-mediated lipid efflux. Amino acid residues 220-231 of the wild-type ApoA-I are required for lipid efflux in vitro and high density lipoprotein formation in vivo. *J Biol Chem.* Feb 28 2003;278(9):6719-6730.

12. Chroni A, Koukos G, Duka A, et al. The carboxy-terminal region of apoA-I is required for the ABCA1-dependent formation of alpha-HDL but not prebeta-HDL particles in vivo. *Biochemistry.* May 15 2007;46(19):5697-5708.

13. Bhattacharyya T, Nicholls SJ, Topol EJ, et al. Relationship of paraoxonase 1 (PON1) gene polymorphisms and functional activity with systemic oxidative stress and cardiovascular risk. *Jama.* Mar 19 2008;299(11):1265-1276.

14. Aviram M, Rosenblat M. Paraoxonases (PON1, PON2, PON3) analyses in vitro and in vivo in relation to cardiovascular diseases. *Methods Mol Biol.* 2008;477:259-276.

15. Rosenblat M, Vaya J, Shih D, et al. Paraoxonase 1 (PON1) enhances HDL-mediated macrophage cholesterol efflux via the ABCA1 transporter in association with increased HDL binding to the cells: a possible role for lysophosphatidylcholine. *Atherosclerosis.* Mar 2005;179(1):69-77.

16. Stevens RC, Suzuki SM, Cole TB, et al. Engineered recombinant human paraoxonase 1 (rHuPON1) purified from Escherichia coli protects against organophosphate poisoning. *Proc Natl Acad Sci U S A.* Sep 2 2008;105(35):12780-12784.

Supplemental Figure 1

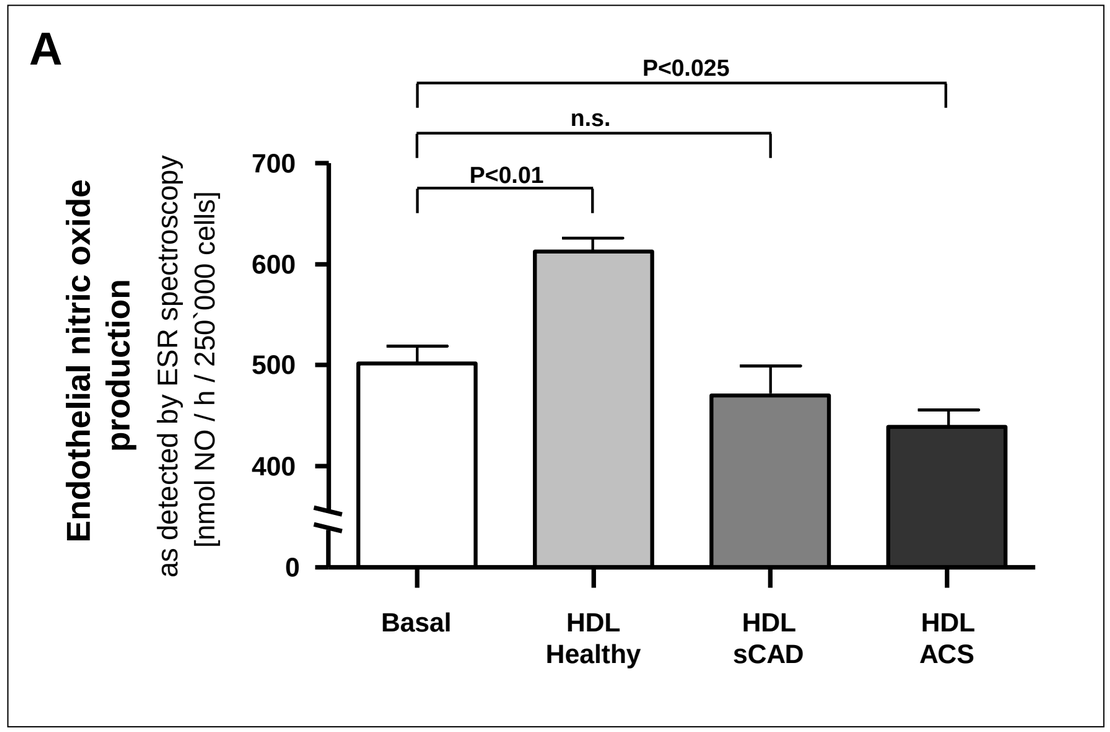

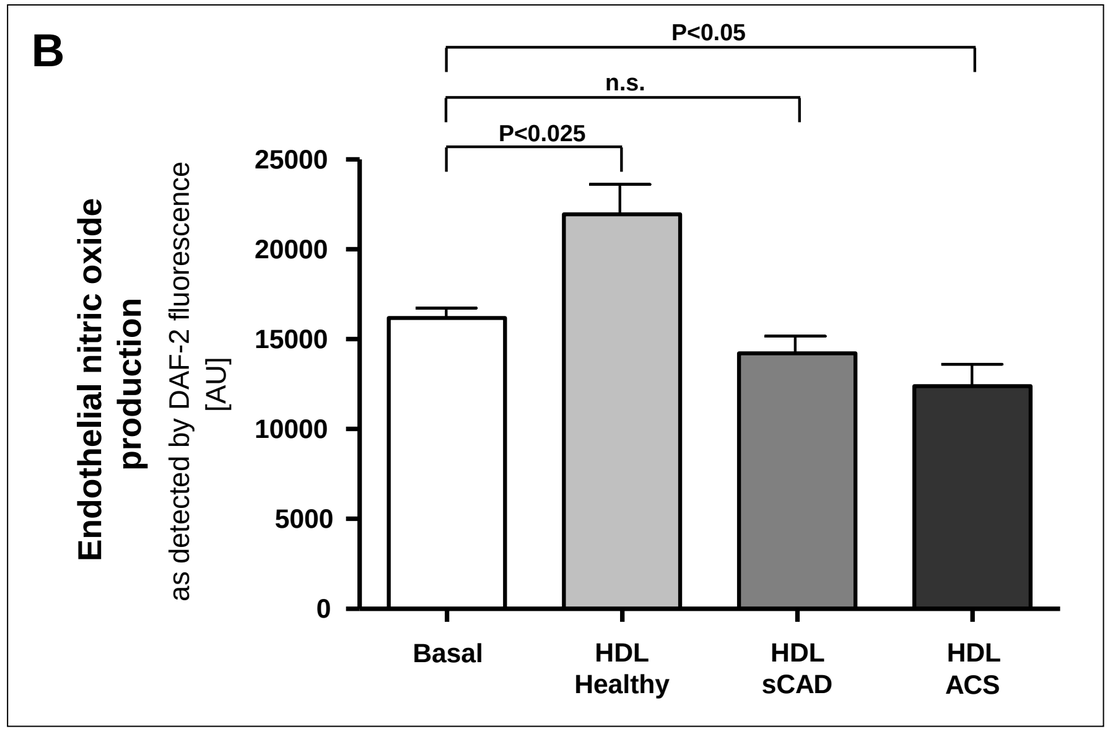

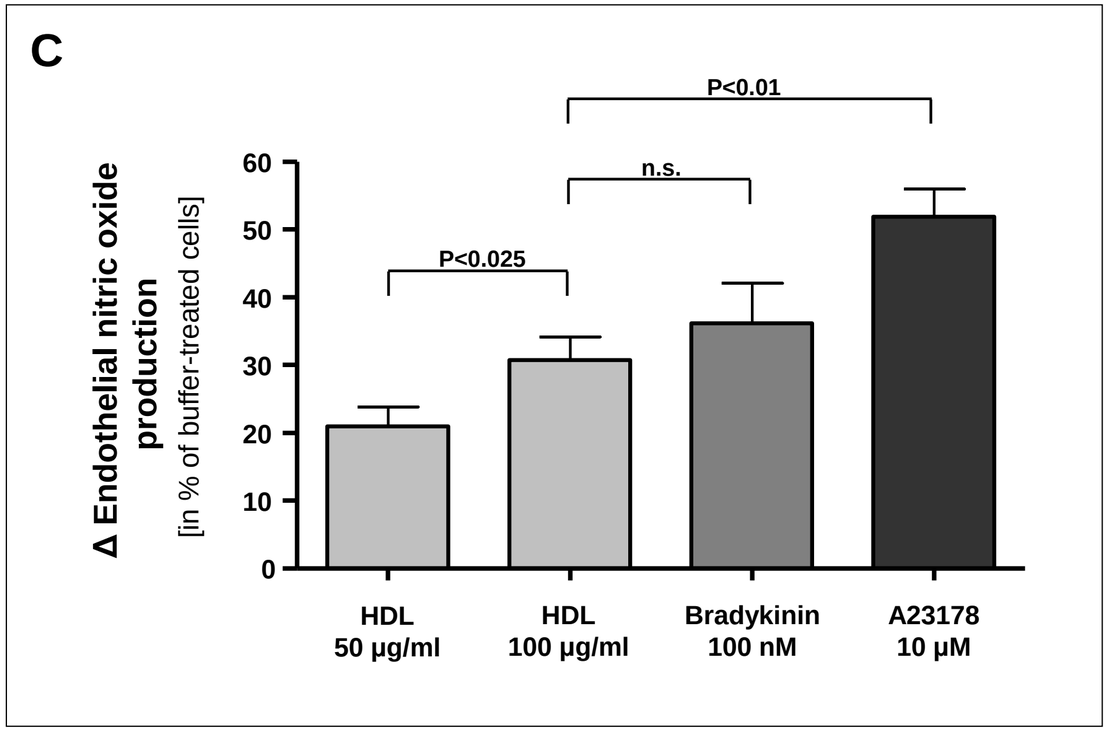

Supplemental Figure 2

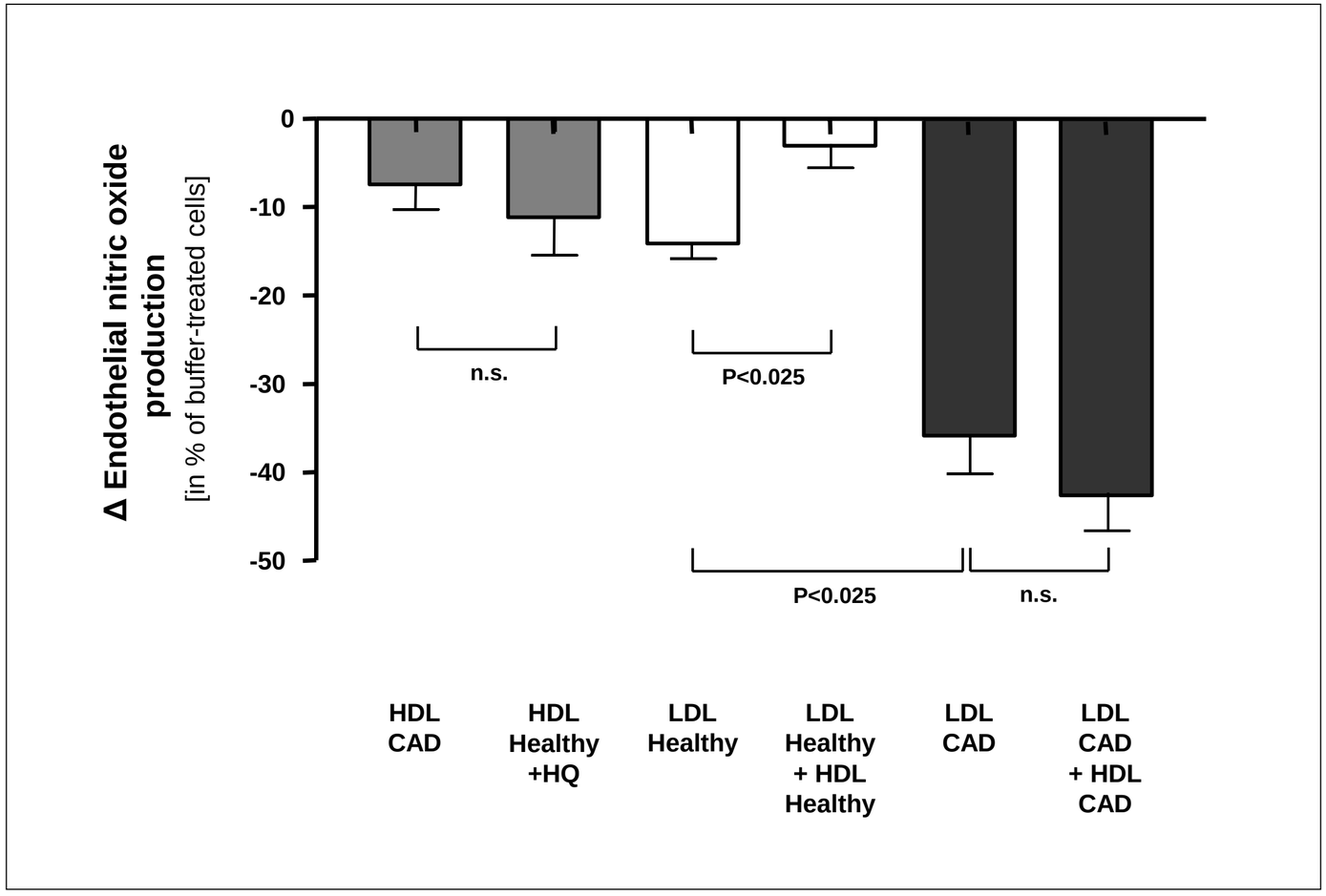

Supplemental Figure 3

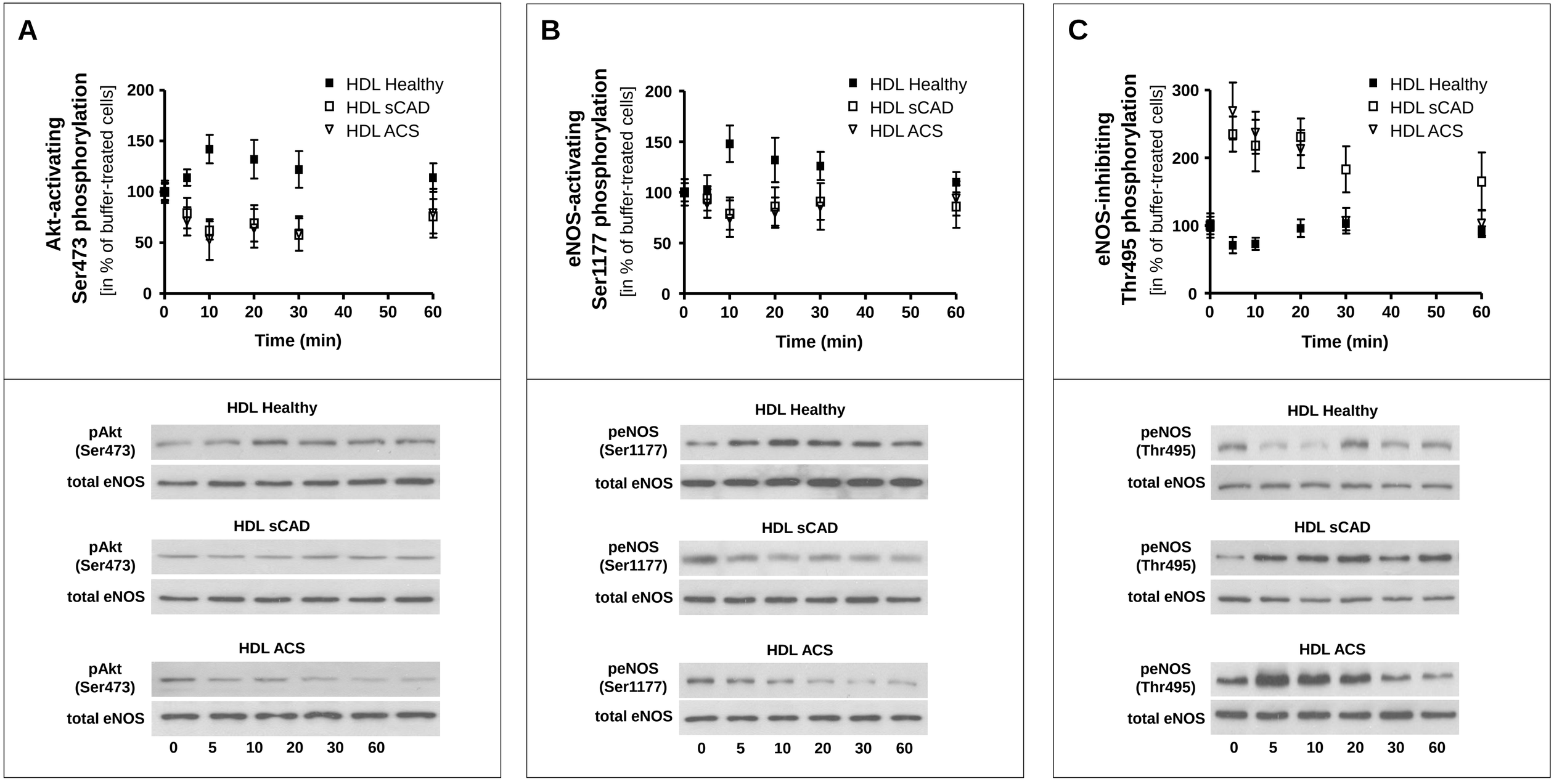

Supplemental Figure 4

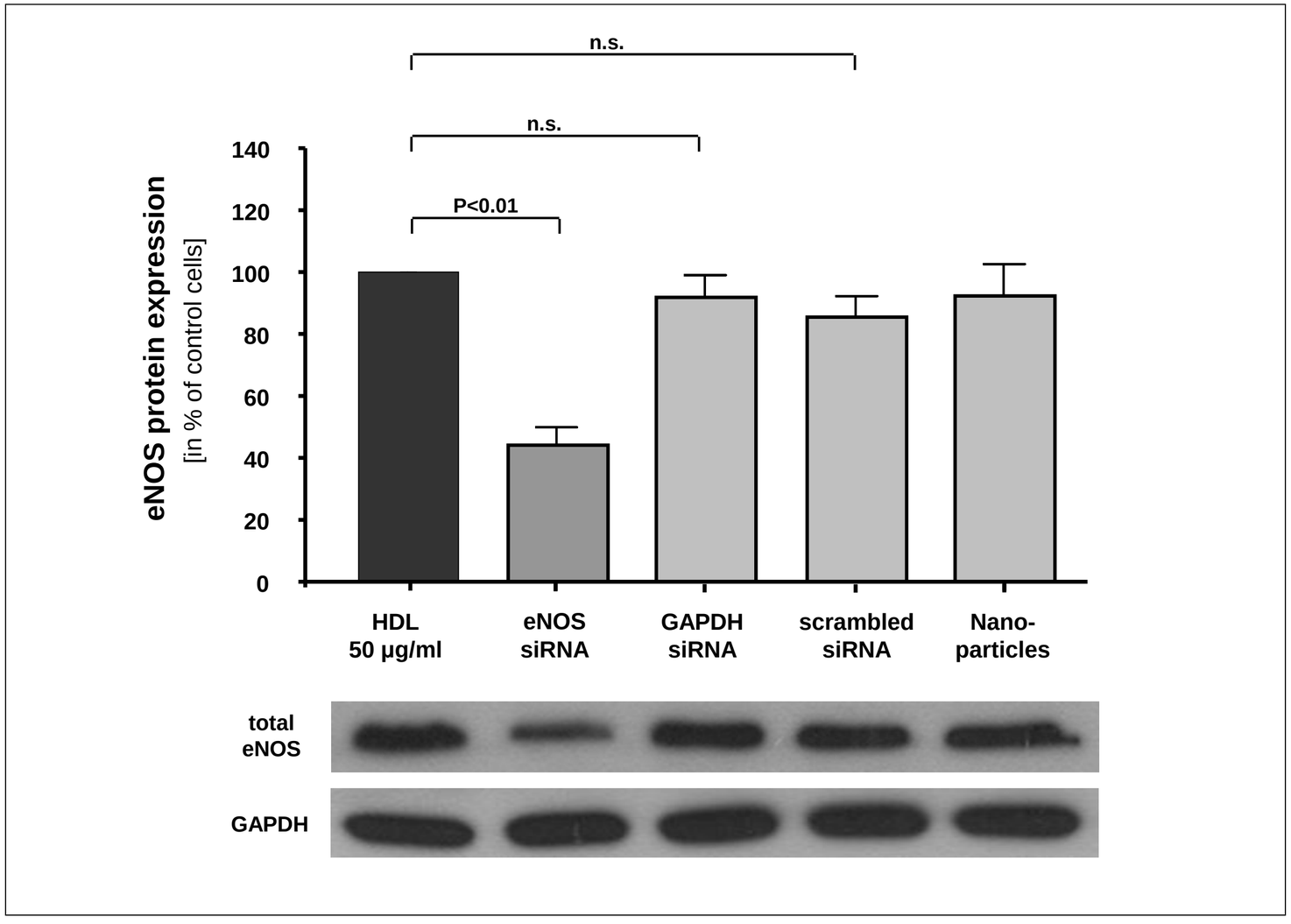

Supplemental Figure 5

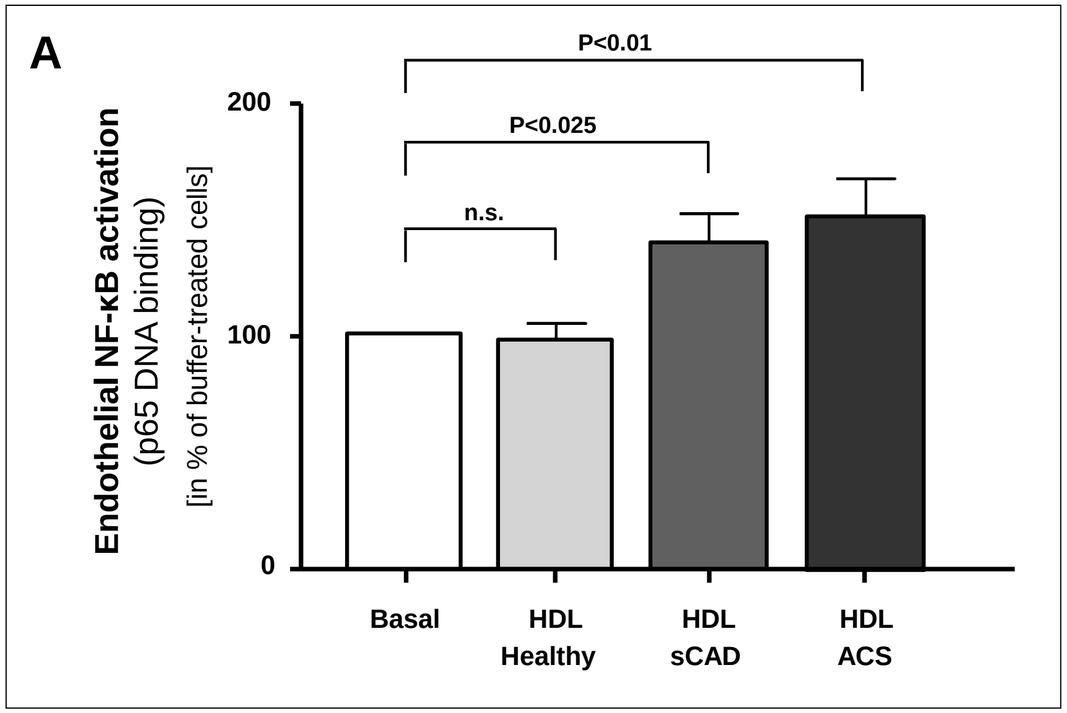

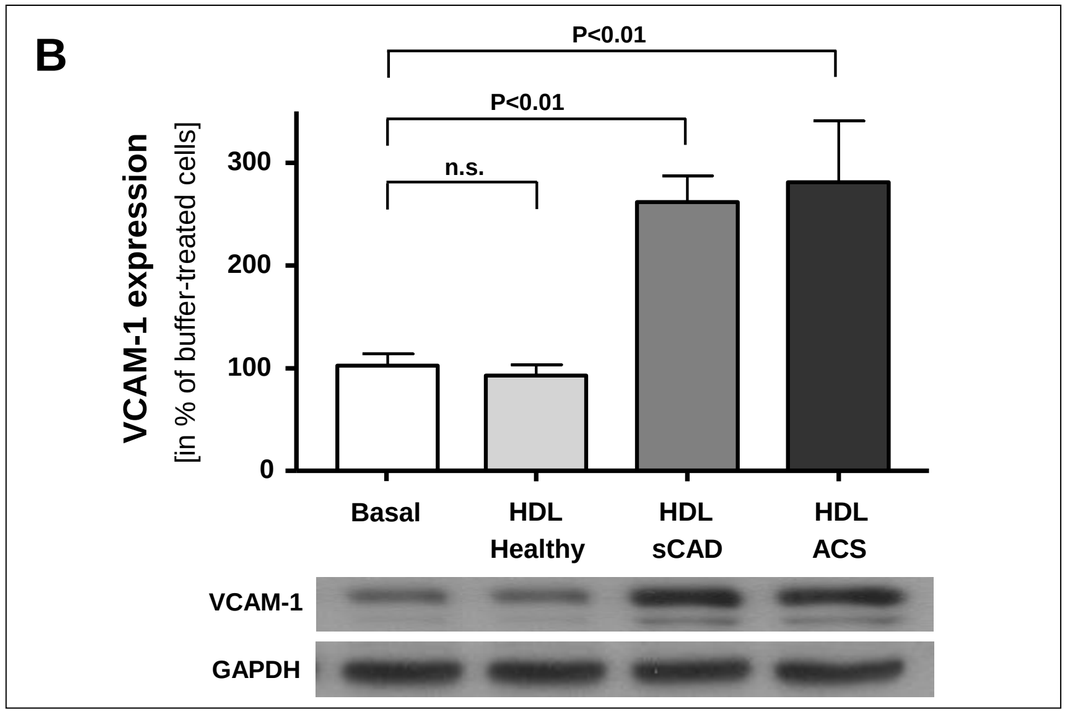

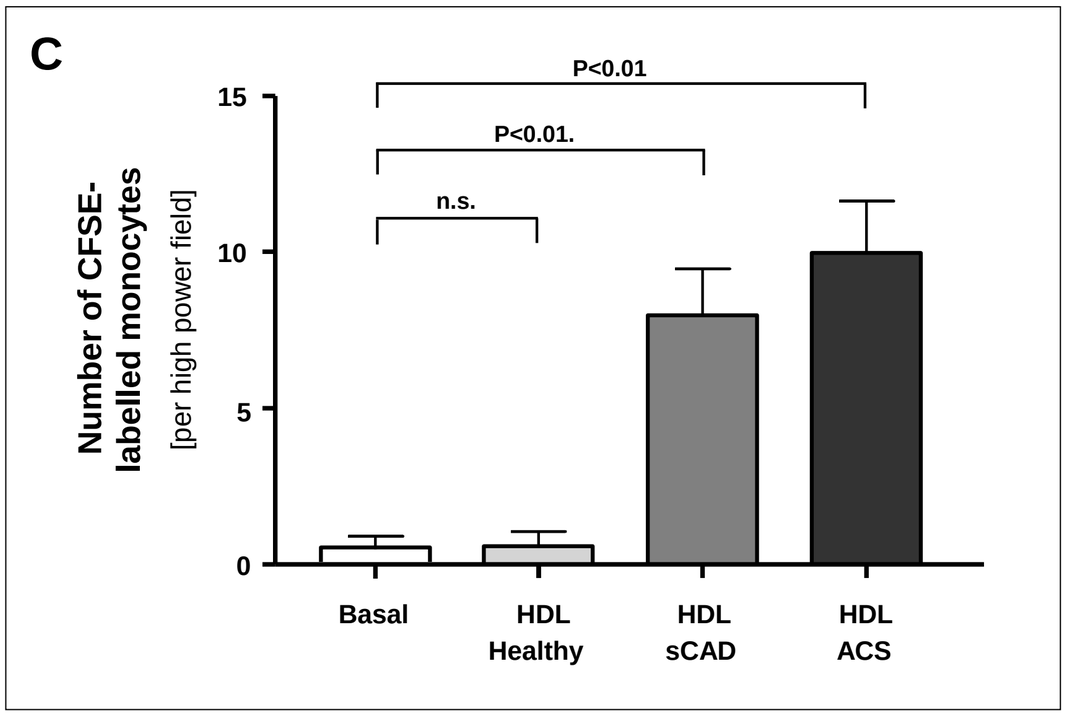

Supplemental Figure 6

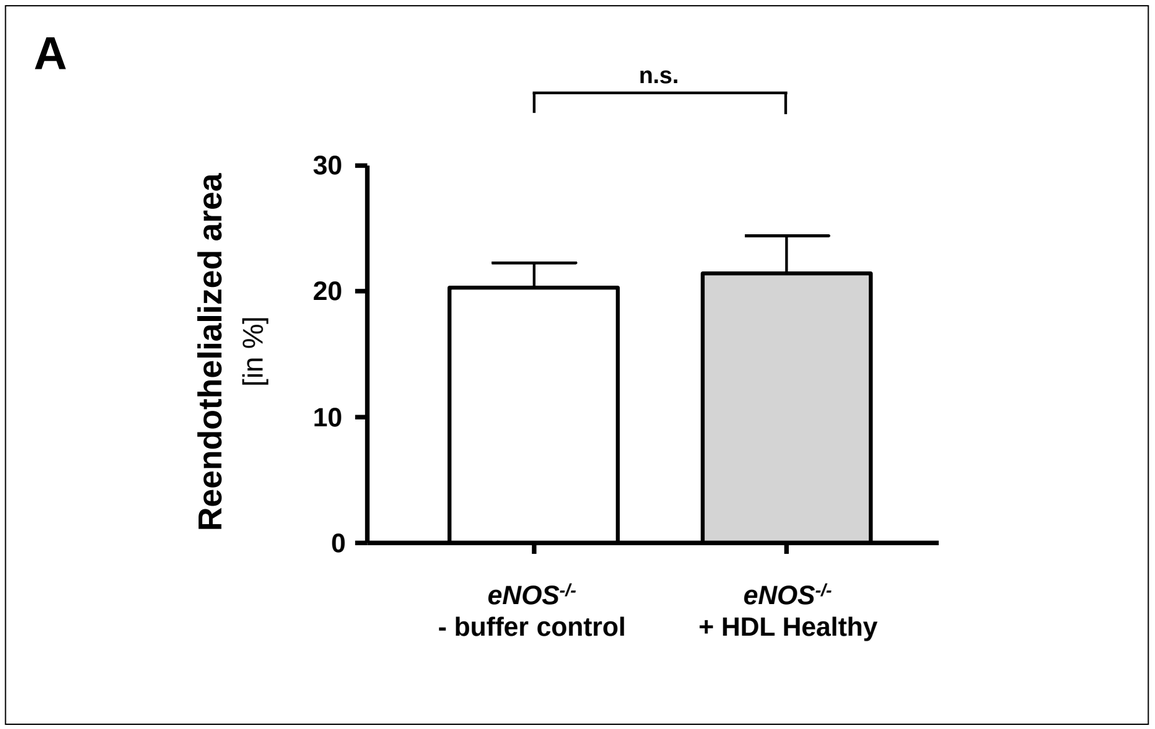

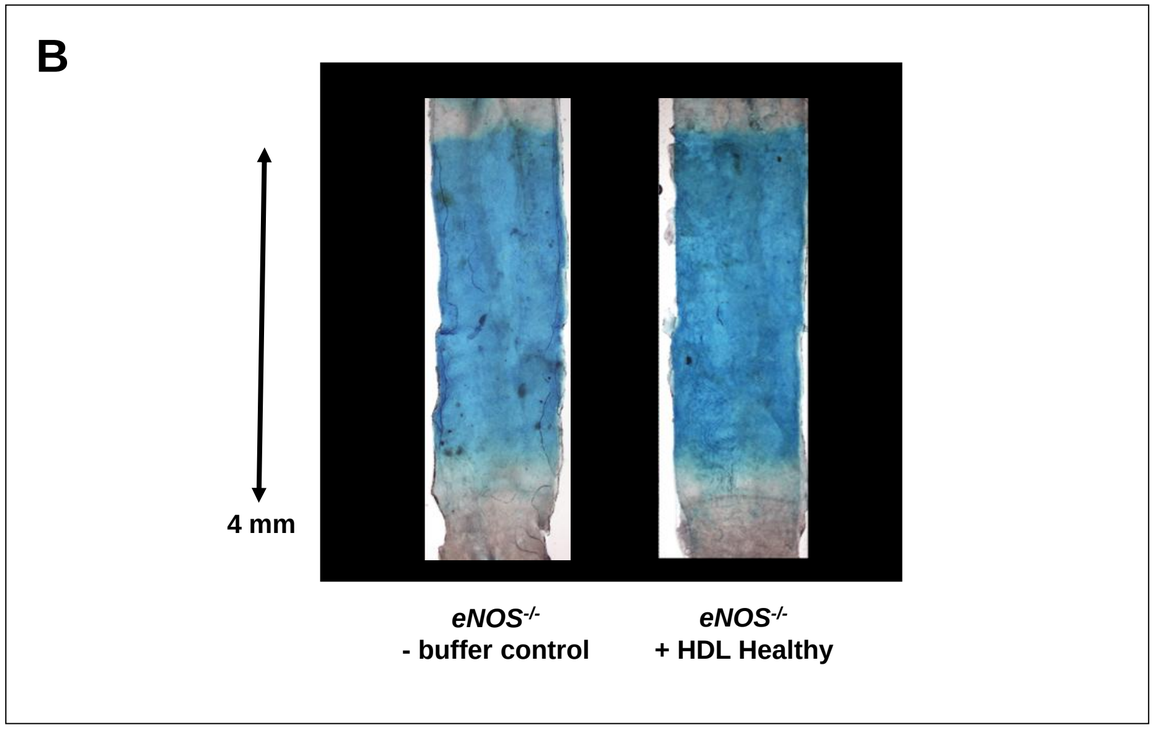

Supplemental Figure 7

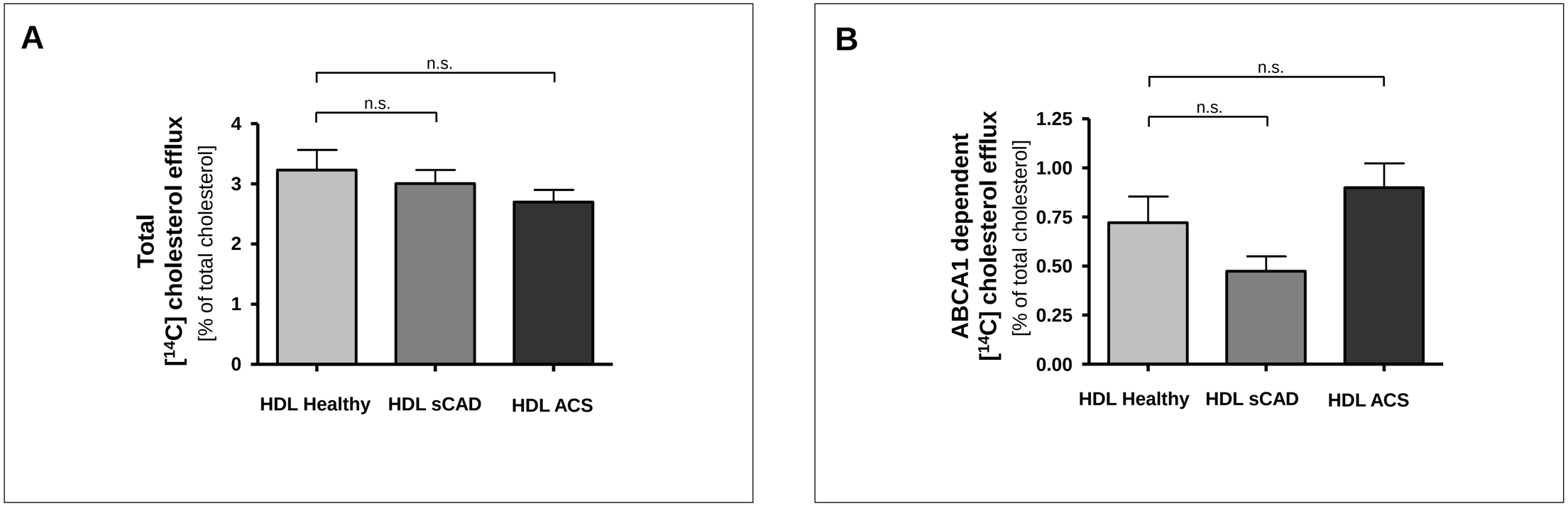

Supplemental Figure 8

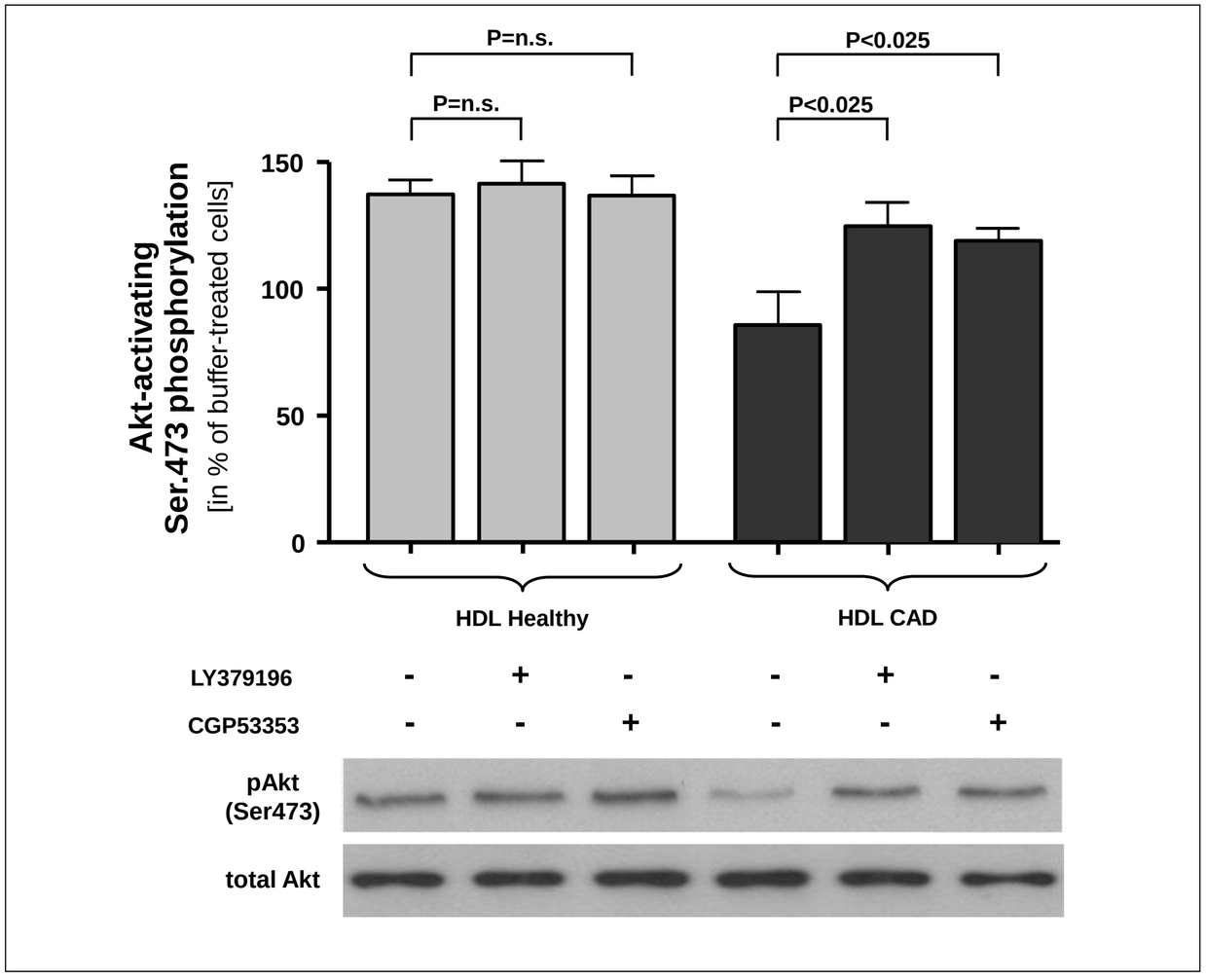

Supplemental Figure 9

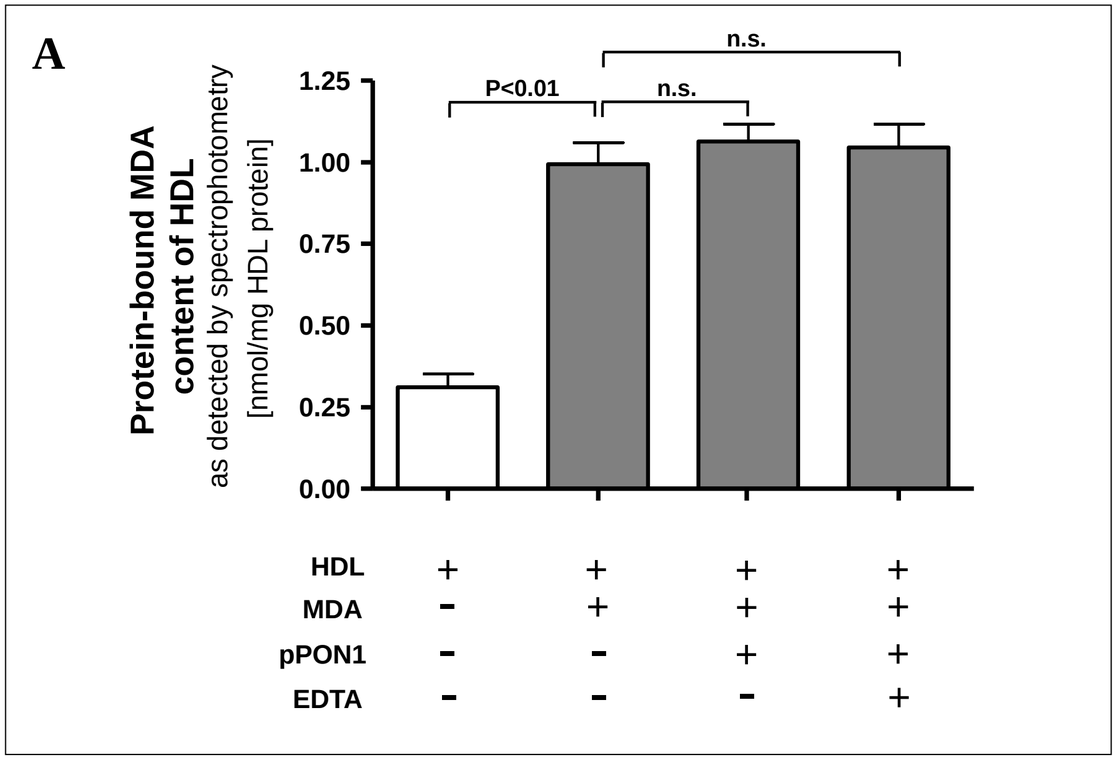

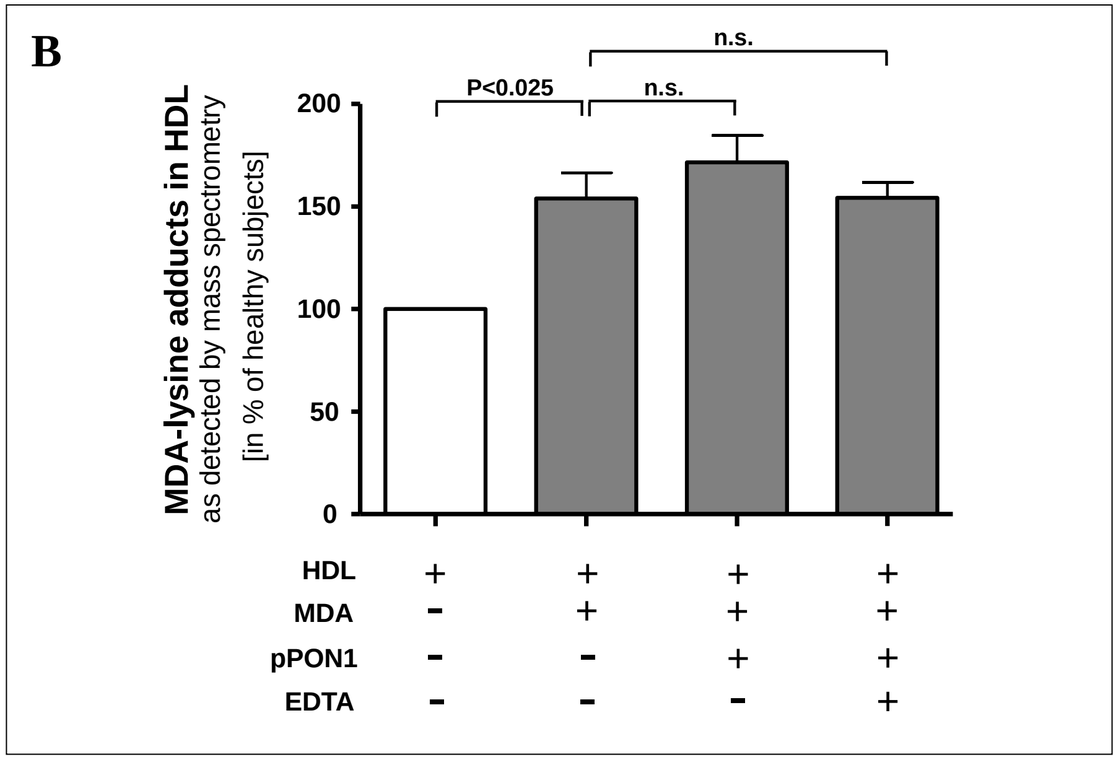

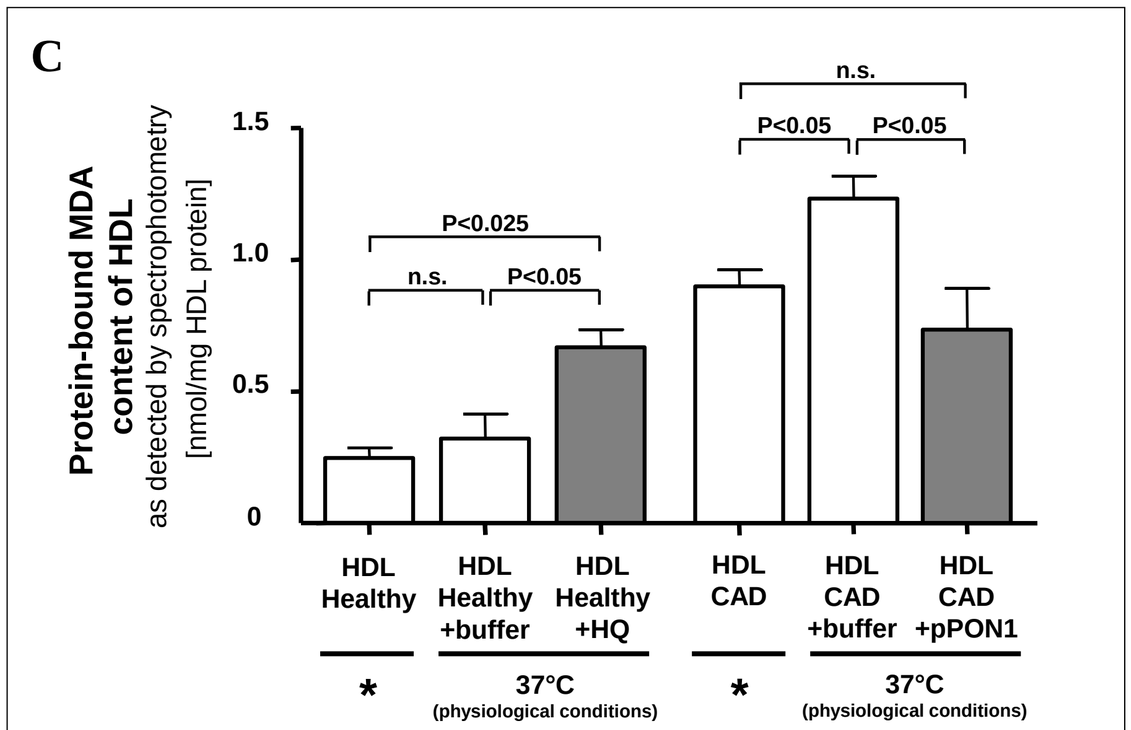

Supplemental Figure 10

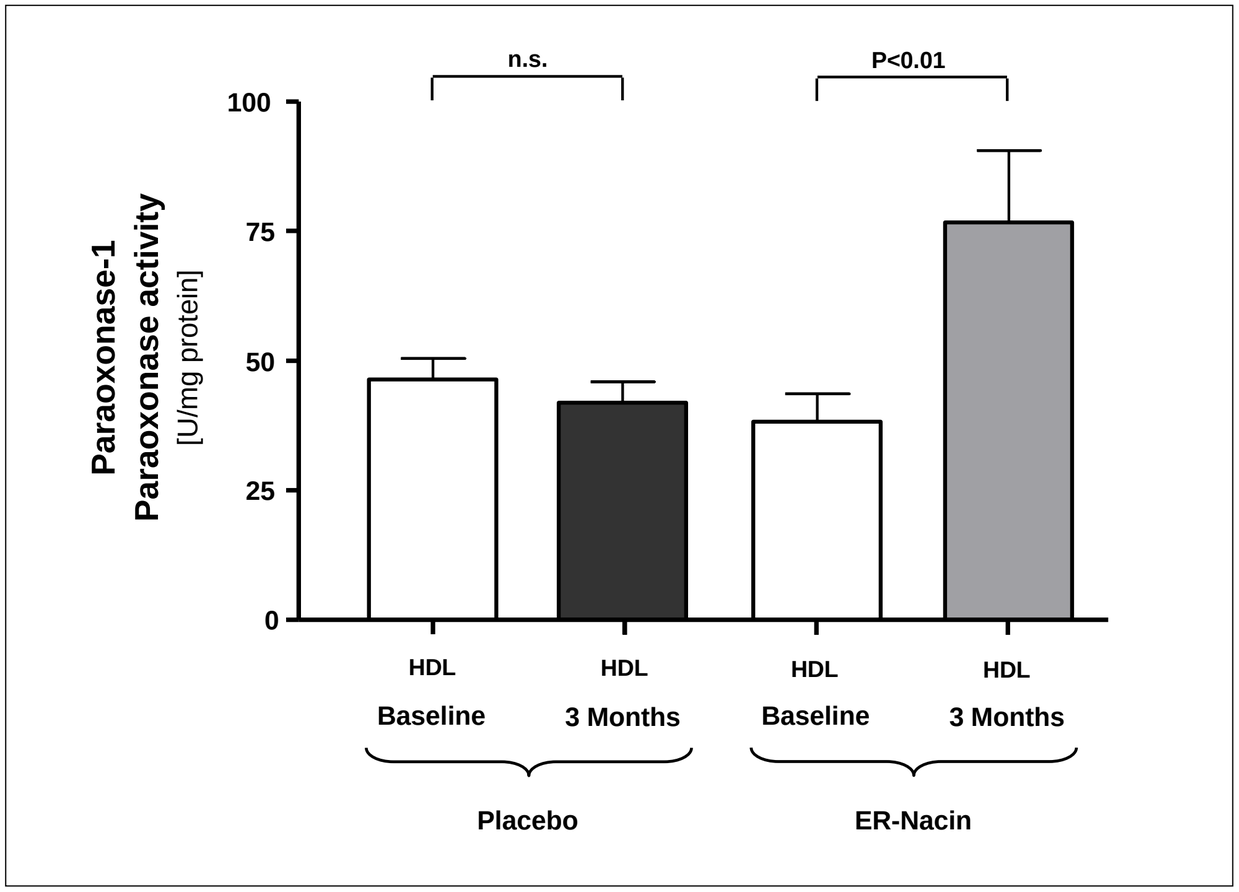

Supplemental Figure 11

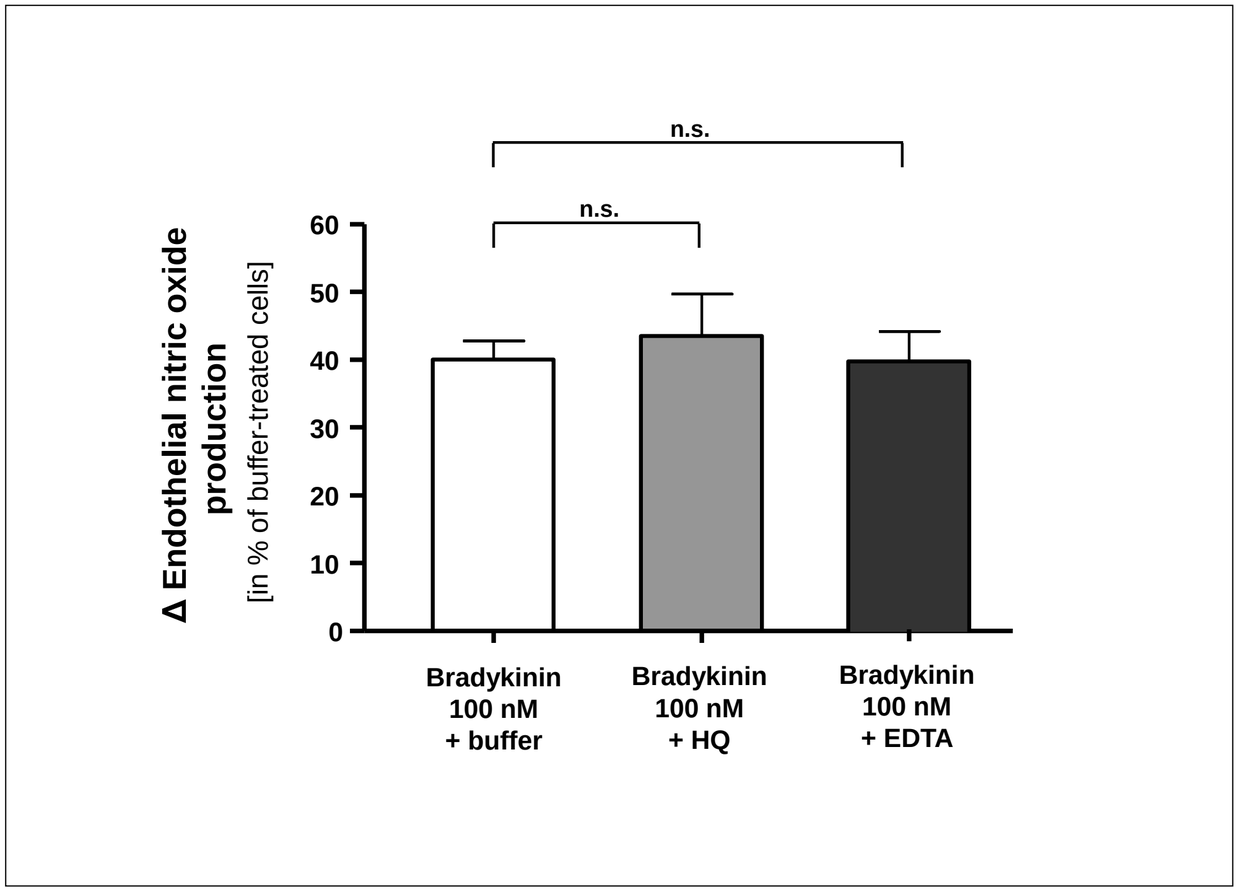

Supplemental Figure 12

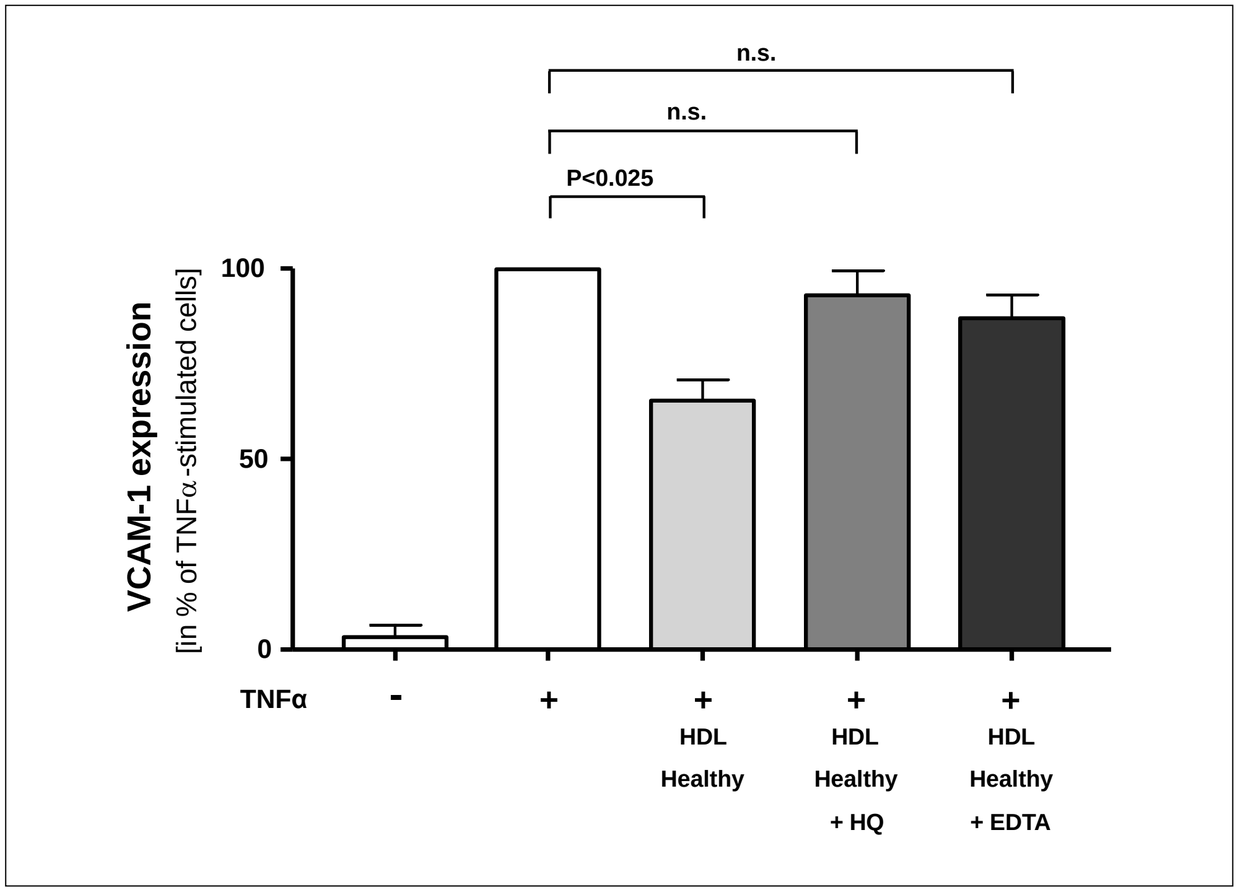

Supplemental Figure 1

Effects of HDL on endothelial NO production as detected by electron spin resonance (ESR) spectroscopy and 4,5-diaminofluorescein diacetate (DAF-2). **(A)** Absolute values of endothelial NO production in endothelial cells incubated for one hour with HDL (50 μg/ml) from healthy subjects, patients with sCAD or ACS, as detected by ESR spectroscopy (in nmol/h/250`000 cells). **(B)** In a subgroup of healthy subjects and patients with stable CAD or ACS (n=8-10 per group), the effects of HDL (50 μg/ml) on nitric oxide production in endothelial cells were also determined by fluorescence staining using DAF-2 as a probe compound for nitric oxide. **(C)** Human aortic endothelial cells were incubated with HDL from healthy subjects (50 and 100 μg/ml), bradykinine (100nM) or calcium ionophore A23178 (10 μM) for one hour and endothelial NO production was determined by ESR spectroscopy (n=8 per group). Data are presented as mean ± SEM.

Supplemental Figure 2

Effects of LDL from healthy subjects and patients with CAD on endothelial NO production as compared to HDL with inhibited PON1 activity. Endothelial cells were exposed to LDL (200 μg/ml) from healthy subjects or patients with CAD, with or without addition of HDL (50 μg/ml). Moreover, endothelial cells were incubated with HDL from patients with CAD or HDL pretreated with the PON1 inhibitor hydroxyquinoline (HQ, 200 μM) and endothelial NO production was measured by electron spin resonance (ESR) spectroscopy. HDL from healthy subjects pretreated with HQ and HDL from patients with CAD had a similar effect on endothelial NO production as compared to LDL from

healthy subjects. Incubation of endothelial cells with LDL from patients with CAD resulted in a significant inhibition of endothelial NO production as compared to LDL from healthy subjects. Notably, HDL from healthy subjects blunted the inhibitory effects of LDL on endothelial NO production, whereas the adverse effects of LDL from patients with CAD were not antagonized by HDL from these patients. Data are presented as mean ± SEM. n=8-12 per group.

Supplemental Figure 3

Time course analysis of the effects of HDL from healthy subjects, patients with sCAD and ACS on endothelial Akt phosphorylation at Ser-473 and eNOS phosphorylation at Ser-1177 and Thr-495. Human aortic endothelial cells were incubated with HDL from healthy subjects, patients with sCAD and ACS for the indicated time points. Phosphorylation of Akt at Ser-473 **(A)** and phosphorylation of eNOS at Ser-1177 **(B)** and Thr-495 **(C)** was determined by Western Blot analysis. Representative blots are shown at the bottom. Data are presented as mean ± SEM. n=10-12 per group.

Supplemental Figure 4

siRNA-specific knockdown of endothelial NO synthase (eNOS) in human aortic endothelial cells. Human aortic endothelial cells were transfected with eNOS-specific, GAPDH-specific or scrambled siRNA using a nanoparticle siRNA transfection system (final siRNA concentration: 15nM) and serum-free cell culture medium. After 24 hours, the effects of siRNA silencing on eNOS protein expression were confirmed by Western Blot. Data are presented as mean ± SEM. n=4 per group.

Supplemental Figure 5

Effect of HDL from healthy subjects, patients with sCAD and ACS on endothelial NF-κB activation, VCAM-1 expression and endothelial monocyte adhesion in non-stimulated endothelial cells. Human aortic endothelial cells were incubated with HDL from healthy subjects, patients with sCAD and ACS (50 μg/ml) for three hours. **(A)** Endothelial NF-κB activation was characterized by detecting the DNA binding of NF-κB subunit p65, as described in the method section (n=10-12 per group). **(B)** The effect of HDL from healthy subjects, patients with sCAD or ACS on basal VCAM-1 expression in endothelial cells was measured by Western Blot (n=8-12 per group) and **(C)** endothelial adhesion of CFSE-labeled human monocytes was detected by fluorescence microscopy (n=8-10 per group). Data are presented as mean ± SEM.

Supplemental Figure 6

Effect of HDL from healthy subjects on endothelial repair in *eNOS*-deficient mice. **(A)** HDL from healthy subjects fails to stimulate re-endothelialization in *eNOS*-deficient mice when compared to buffer control (n=6 per group). **(B)** Representative photographs of carotid arteries from *eNOS*-deficient mice stained with Evan`s Blue. Data are presented as mean ± SEM.

Supplemental Figure 7

Effects of HDL from healthy subjects, patients with sCAD and ACS on total, ABCA1 and ABCG1-dependent cholesterol efflux. **(A)** The capacity of HDL (10μg/ml apoA-I)

from healthy subjects and patients with sCAD or ACS to stimulate total cholesterol efflux was measured in untreated J774 macrophages. **(B)** ABCA1-dependent cholesterol efflux capacity of HDL was detected in J774 macrophages treated with the cAMP analog cpt-cAMP, that upregulates ABCA1. **(C)** ABCG1-dependent cholesterol efflux capacity of HDL (28µg/ml apoA-I) was measured in HEK293 cells transfected with an ABCG1-expressing plasmid or a mock plasmid. n=15 per group, data are presented as mean ± SEM.

Supplemental Figure 8

Role of PKCßII activation for altered effects of HDL from patients with CAD on endothelial Akt phosphorylation at Ser-473. Incubation of endothelial cells with LY379196, a nonselective inhibitor of PKCßI and PKCßII isoforms, and CGP53353, a highly selective inhibitor of PKCßII, partly restored the ability of HDL from patients with CAD to stimulate the activating Akt phosphorylation at Ser-473 (n=8-10 per group). Data are presented as mean ± SEM.

Supplemental Figure 9

Effect of purified PON1 on MDA content and MDA-lysine adducts in MDA-modified HDL. HDL (200 µg protein/ml) was incubated with MDA (12.5 mol MDA/mol apoA-I) for 24 hours at 37°C and, subsequently, MDA-modified HDL was incubated for an additional 6 hours with purified (p)PON1 (5 Units/100µg HDL protein) with or without EDTA (5 mM) at 37°C. Afterwards, the protein-bound MDA content in HDL **(A)** was analyzed by spectrophotometry and the MDA-lysine adducts in HDL **(B)** were detected

by mass spectrometry. **(C)** Moreover, the protein bound MDA content was measured in HDL from healthy subjects and patients with CAD immediately after isolation (*) and after incubation of HDL with the PON1 inhibitor hydroxyquinoline (HQ, 200 µM) for 6 hours at 37°C. Data are presented as mean ± SEM.

Supplemental Figure 10

Effect of extended-release niacin therapy on HDL-associated PON1 activity in patients with metabolic syndrome and low plasma HDL cholesterol levels. HDL was isolated from patients with metabolic syndrome and low plasma concentration of HDL cholesterol before and after 3 months of ER niacin therapy (n=15) or placebo (n=15) by ultracentrifugation. HDL-associated PON1 activity was measured by UV-spectrophotometry, as described in detail in the method section. Data are presented as mean ± SEM.

Supplemental Figure 11

Effect of dialyzed hydroxyquinoline (HQ) and EDTA preparations on bradykinine-induced endothelial nitric oxide production. Dialyzed HQ and EDTA samples were prepared according to the protocol that was used for inhibition of HDL-associated PON1 (see method section for details). Human aortic endothelial cells were incubated with buffer or dialyzed HQ or EDTA samples and the effect of bradykinine on endothelial NO production was measured by electron spin resonance (ESR) spectroscopy (n=4-5 per group). Data are presented as mean ± SEM.

Supplemental Figure 12

Effect of inhibition of HDL-associated PON1 on endothelial VCAM-1 expression. Treatment of HDL from healthy subjects with PON1 inhibitors impaired the capacity of HDL to inhibit TNF-α stimulated VCAM-1 expression in human aortic endothelial cells, as detected by Western Blot (n=8-10). Data are presented as mean ± SEM.